SLAC-PUB-1329
(T/E)
October 1973

HADRONIC AND ELECTROMAGNETIC INTERACTIONS AT LARGE TRANSVERSE MOMENTUM*

Stanley J. Brodsky
Stanford Linear Accelerator Center
Stanford University, Stanford, California 94305

ABSTRACT

The scaling laws of inclusive and exclusive processes at large transverse momentum are reviewed. Their theoretical interpretation in terms of composite models for the hadrons is then discussed. The observed inverse power-law behavior of the invariant cross sections at fixed invariant ratios is found to agree with the degrees of freedom suggested by the simple dimensional counting in the quark model. Such counting is characteristic of renormalizable quark field-theoretic models with asymptotically scale-invariant constituent interactions and finite Bethe-Salpeter wavefunctions. However, as suggested by the parton interchange model, elementary gluon interactions between quarks of different hadrons must be suppressed in order to understand (1) the scaling, but not scale-invariant behavior of the inclusive hadronic cross section for meson production at large transverse momentum, and (2) the effective Regge behavior at large t and angular distribution of exclusive hadronic and electromagnetic processes.

INTRODUCTION

If any aspect of hadron physics could be simple — reflecting the properties of underlying basic interactions at short distances — then it must be collision processes involving particle production at large transverse momentum. Recent measurements from the ISR[1-3] and NAL[4] show that the inclusive cross sections for hadron production at large transverse momentum are much larger than that expected from an exponential extrapolation of small $p_\perp$ data. Moreover, the striking pattern of scaling laws observed in both exclusive and inclusive data at large $p_\perp$ has given strong support to quark-parton field theoretic models of composite hadrons, and a clearer picture of the underlying dynamics of the constituents is now beginning to emerge.

Let us begin with a review of the scaling laws of the large transverse momentum experiments. For inclusive processes we have:

(1) The Bjorken scaling[5] of deep inelastic lepton scattering:[6]

* Work supported in part by the U.S. Atomic Energy Commission.

(Invited talk presented to the Fifth International Conference on High Energy Collisions, Stony Brook, N. Y., August 1973)

$$\frac{d\sigma}{d^3p/E}(ep \to eX) \to \frac{1}{s^2} f\left(\frac{t}{s}, \frac{\mathcal{M}^2}{s}\right) \qquad (1)$$

$$s \to \infty, \quad t/s, \quad \mathcal{M}^2/s \text{ fixed}.$$

This displays the remarkable scale invariance of the invariant cross section: The mass scale is irrelevant! Here $t = (p_e - p_e')^2 = q^2$ and $\mathcal{M}^2$ is the square of the invariant missing mass. To the extent that this scale invariance holds experimentally we can deduce (in one photon exchange approximation) that the structure functions $W_1(p\cdot q, q^2)$ and $\nu W_2(p\cdot q, q^2)$ are only a function of $\omega = -2p\cdot q/q^2 = (\mathcal{M}^2 - t)/(-t)$, and infer that the electromagnetic interactions within hadrons are scale invariant.

(2) The scaling law of large transverse momentum meson production: The result of the CERN-Columbia-Rockefeller[1] collaboration is (see Fig. 1)

$$\frac{d\sigma}{d^3p/E}(pp \to \pi^o X) = \frac{1}{p_\perp^N} \Gamma(p_\perp/\sqrt{s}) \qquad (2)$$

$$\text{for } 3 \text{ GeV} < p_\perp < 9 \text{ GeV},$$

$$23.5 \text{ GeV} < \sqrt{s} < 62.4 \text{ GeV}, \text{ and } \Theta_{CM} \cong 90^o \ (p_\ell^{CM}/\sqrt{s} \cong 0).$$

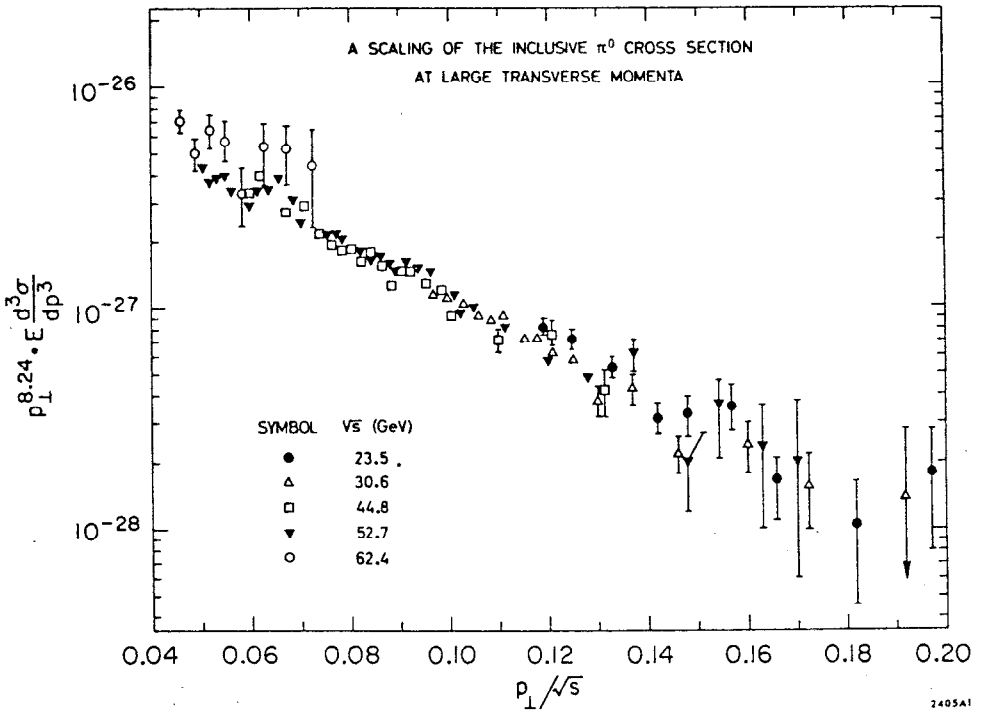

FIG. 1 — The scaling behavior of the cross section $pp \to \pi^o X$ at large transverse momenta measured by the CERN-Columbia-Rockefeller collaboration, Ref. 1.

A value for N could be chosen such that $\Gamma = p_\perp^N \, d\sigma/(d^3p/E)$ is independent of s for any value of $p_\perp/\sqrt{s}$. The best fit is $N = 8.24 \pm 0.05$.[7] Also, a useful representation for the $p_\perp/\sqrt{s}$ dependence is

$$\Gamma = \exp(-c\, p_\perp/\sqrt{s}) \tag{3}$$

with $c = 26.1 \pm 0.5$. In terms of invariants, we thus have

$$\frac{d\sigma}{d^3p/E}(pp \to \pi^o X) \to \frac{1}{s^{N/2}} f\left(\frac{t}{s}, \frac{\mathcal{M}^2}{s}\right) \tag{4}$$

$$s \to \infty, \quad t/s, \quad \mathcal{M}^2/s \text{ fixed}$$

where $N/2 \sim 4$. In contrast to deep inelastic electron scattering, the invariant cross section displays scaling but is not asymptotically scale invariant. These results seem to be consistent also with recent data for $pp \to \pi^+X$ measured at NAL[4], and data at lower $p_\perp$ measured by the British-Scandinavian collaboration at the ISR.[3]

The form of Eq. (4) (but with N = 4) was first predicted by Berman and Jacob[8] and Berman, Bjorken, and Kogut.[9] The scaling law with N = 8 is a prediction of the parton interchange model developed by Blankenbecler, Gunion, and myself.[10,11] [See also Refs. 12 and 13.]

Scaling laws at large transverse momentum are also a feature of exclusive processes. In fact, in each case of hadron-hadron scattering and also pion photoproduction, one finds the differential cross section interpolates smoothly between the exponentially falling peaks at t = 0 and u = 0. Away from the forward and backward regions, one finds the invariant cross sections are consistent with the scaling law:[10,12]

$$\frac{d\sigma}{dt} \to \frac{1}{s^N} f(t/s) \tag{5}$$

$$s \to \infty, \quad t/s \text{ fixed}$$

i.e.: $s^N \, d\sigma/dt = f(\cos\theta_{CM})$ is a universal function independent of s. The energy independence of $(d\sigma/dt)/(d\sigma/dt)|_{90^o}$ of pp scattering and Kp scattering is shown in Figs. 2 and 3.

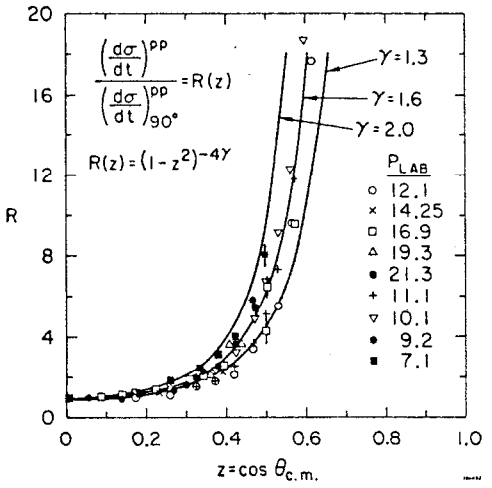

FIG. 2 — The angular distribution of pp scattering at large CM angles (from Ref. (10). The energy independence of R(z) is a property of the exclusive scattering scaling law. The curves show various possible fits to the angular dependence.

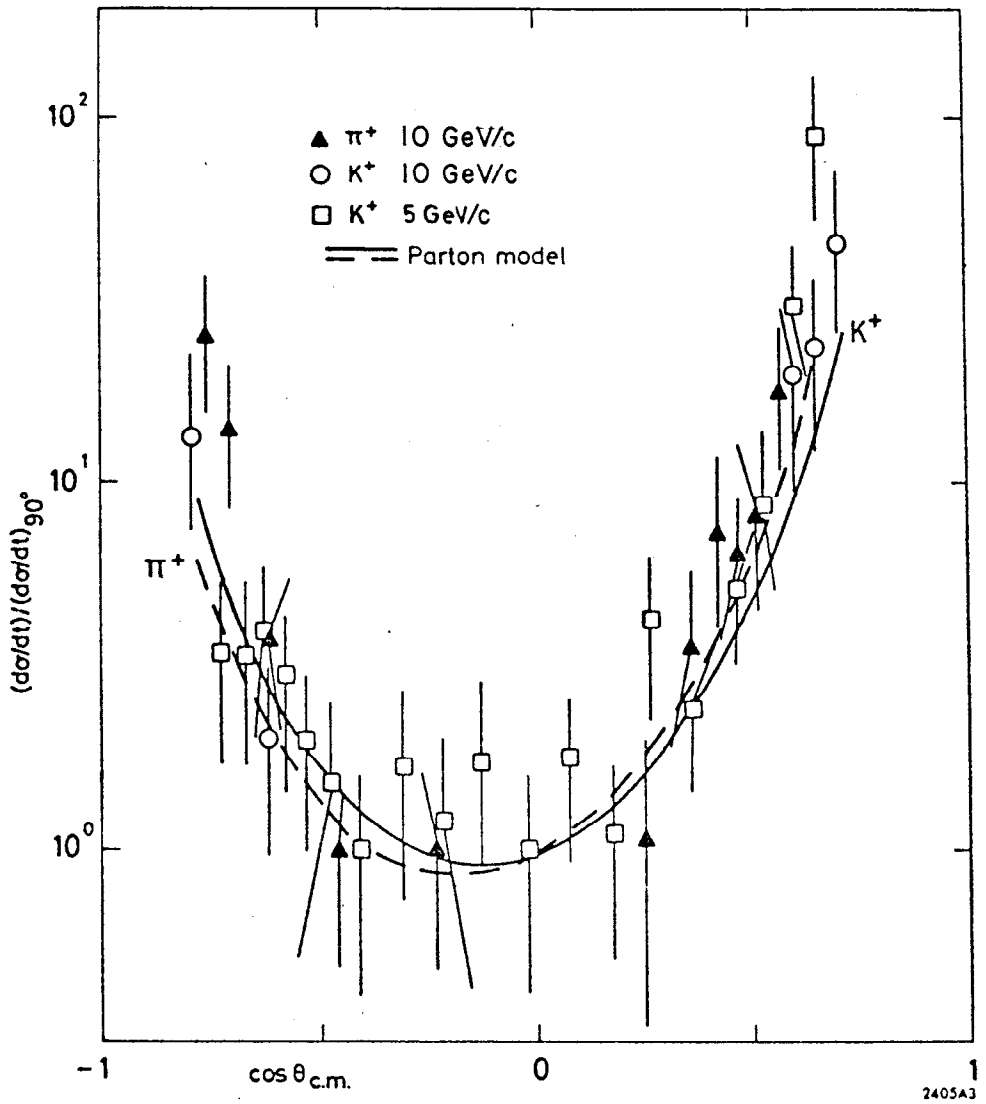

FIG. 3 — The angular dependence of $\pi^+ p \to \pi^+ p$ and $K^+ p \to K^+ p$ scattering (from Ref. 14). The curves are the predictions of the parton-interchange model of Ref. 10.

The exclusive scaling laws are an extremely rich source of information since the power of N and the functional dependence of f(t/s) depends on the nature of the interacting hadrons. The fit to pp scattering shown in Fig. 4 by Landshoff and Polkinghorne[15] gives $N_{PP} = 9.7 \pm 0.5$ (although the points at the highest values of s and t may indicate a higher power[10]). On the other hand, in the case of meson-baryon scattering, the data appear to cluster near N = 8 [See Fig. 5]:

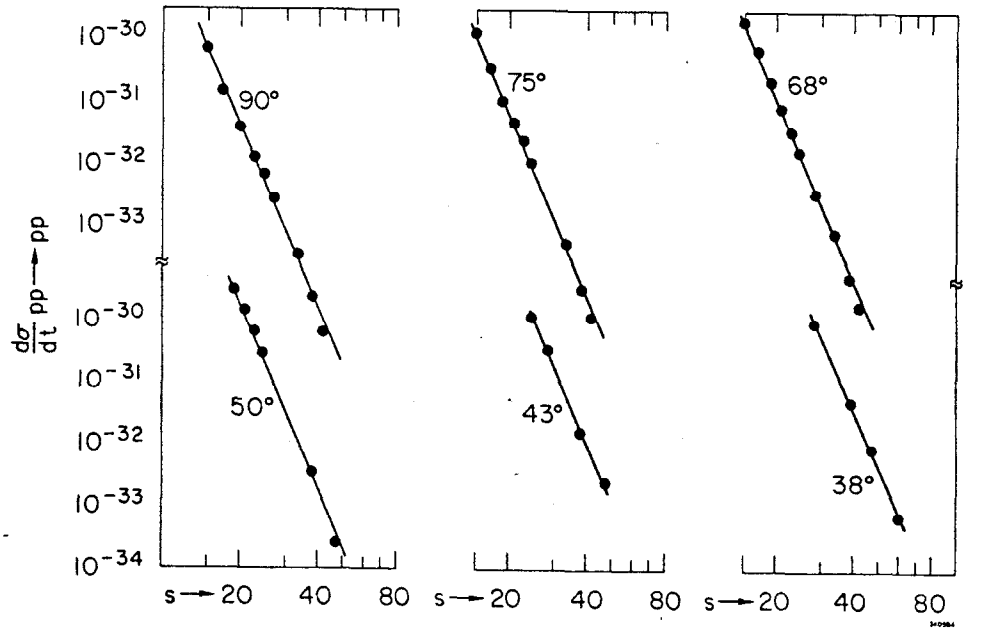

FIG. 4 — The energy dependence of pp scattering at different CM angles (from Ref. 15).

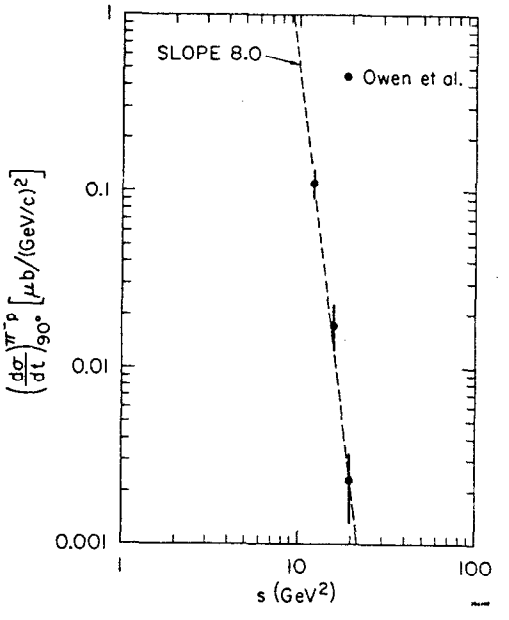

FIG. 5 — The energy dependence[10] of $\pi^- p$ scattering at 90^0. The data are from Ref. 16.

$$N_{MB} = \begin{cases} 8 \pm 1 & \pi^- p \to \pi^- p \quad 16 \\ 7 \pm 1 & \pi^+ p \to \pi^+ p \quad 14 \\ 8 \pm 1 & K^+ p \to K^+ p \quad 14 \\ 8.5 \pm 1.4 & K_L p \to K_S p \quad 17 \\ 7.4 \pm 1.4 & K_0 p \to \pi^+ \Lambda \quad 17 \\ 8.1 \pm 1.4 & K_0 p \to \pi^+ \Sigma \quad 17 \end{cases} \tag{6}$$

In the case of pion-photoproduction $\gamma p \to \pi^+ n$ a recent measurement at SLAC[18] gives $N = 7.3 \pm 0.4$.

An essential feature of the large angle exclusive data is the behavior of the effective trajectories at large momentum transfer. If one fits the amplitude to the form $\mathcal{M} = s^{\alpha(t)} \beta(t)$ or $u^{\alpha(t)} \beta(t)$, then $\alpha(t)$ is found to be negative at large t. As we shall argue later, this indicates the absence

of leading processes involving elementary gluon exchange between the hadrons which give fixed singularities at $J \sim 1$ or at $J = 0$ in the hadronic amplitudes.

In the case of elastic electron-nuclear scattering or $e^+e^- \to \pi^+\pi^-$, K^+K^-, a related type of power law scaling at fixed t/s is observed. The results are consistent with a proton form factor satisfying asymptotically[19] $F_{1p}(t) \sim t^{-2}$, $F_{2p} \sim t^{-3}$ (i.e. G_E/G_M scaling), and the meson form factor behaving as $1/t^{1.08 \pm 0.15}$. This last result is the fit to the cross section for $e^+e^- \to \pi^+\pi^-$, K^+K^- measured at Frascati.[20]

The observation of these scaling laws at large transverse momentum for both exclusive and inclusive processes is a fascinating challenge to theory and leads us to some fundamental questions: Do these scaling laws reflect the properties of basic interactions at short distances? Do the power behavior and degrees of freedom indicated by the scaling laws imply that the hadrons are composites of quark-parton fields? In the remainder of this talk, I will describe some recent theoretical approaches to large transverse momentum processes which I have worked on in collaboration with Dick Blankenbecler, Jack Gunion, and Bob Savit, and also with Glennys Farrar. On the basis of this work, the answers to these questions appear to be in the affirmative, and strong clues to the existence and properties of a microscopic theory of the hadrons seem to be emerging.

THEORETICAL MODELS FOR EXCLUSIVE PROCESSES AT LARGE TRANSVERSE MOMENTUM

Decreasing electromagnetic form factors and Bjorken scaling strongly suggest a composite field-theoretic model for the hadrons. In fact, as has been shown in the parton interchange model[10], all of the above scaling laws can emerge as a natural consequence of constituent models. Further, the power dependence of the scaling laws, and in fact the form of the functions $f(t/s)$ and $f(t/s, \mathcal{M}^2/s)$, can be connected via wavefunction models to the power dependence of the hadronic form factors.

First, however, I would like to discuss a new approach done in collaboration with Glennys Farrar which allows the power behavior of the scaling laws to be computed directly from an underlying field theory. We make the following assumptions:

(A) The mesons and baryons are Bethe-Salpeter bound states of two and three quark fields respectively. Thus in the limit of zero binding, the hadrons would become free quark states:

$$\begin{aligned} |B\rangle &\to |qqq\rangle \\ |M\rangle &\to |q\bar{q}\rangle \end{aligned} \tag{7}$$

Also, as discussed below, we assume a simple, physical limit on the high momentum components in the wavefunction.

(B) The interactions of the hadronic constituents are asymptotically scale invariant, as implied by Bjorken scaling.

With these assumptions we then obtain for large angle scattering of hadrons, photons, and leptons, the scaling law [21]

$$\frac{d\sigma}{dt} \Rightarrow s^{-(2+N_M+2N_B)} f(t/s) \tag{8}$$

$$s \to \infty, \quad t/s \text{ fixed} .$$

Here N_M and N_B are the total number of mesons and baryons in the initial and final state. Thus at fixed t/s or $\cos\theta_{CM}$ we obtain

$$\frac{d\sigma}{dt} \to \begin{cases} s^{-10} & pp \to pp, \text{ etc.} \\ s^{-8} & \pi p \to \pi p, Kp \to Kp, \text{ etc.} \\ s^{-7} & \gamma p \to \pi p \end{cases} \tag{9}$$

which are all consistent with experiment. We also predict

$$\frac{d\sigma}{dt} \to \begin{cases} s^{-6} & \gamma p \to \gamma p \\ s^{-7} & \gamma p \to \rho p \\ s^{-4} & \gamma\gamma \to \pi\pi \quad . \end{cases} \tag{10}$$

Applying the scaling law to elastic-electron scattering, one finds for the (spin-averaged) form factors, $F(t) \to t^{-(n_q-1)}$ where n_q is the number of quark fields in the hadrons. Thus for large t,

$$F_{1p}(t) \sim t^{-2}, \quad F_{2p} \sim t^{-3} ,$$
$$F_\pi \sim t^{-1}, \quad F_K \sim t^{-1} , \tag{11}$$

and $F(t) \sim t^{-5}$ for the deuteron. All of these results could be modified by a finite number of logarithms. A similar scaling result for elastic processes has been obtained independently by Matveev, Muradyan, and Tavkhelidze[22] using a scale-invariance argument.

More generally, for any exclusive strong or electromagnetic process at fixed CM angle, dimensional scaling gives[21]

$$\Delta\sigma = \frac{1}{s^{1+N_M+2N_B}} f\left(\frac{p_i \cdot p_j}{s}\right) , \text{ (mod log s)} \tag{12}$$

$$\text{for } s \to \infty, \quad p_i \cdot p_j/s \text{ fixed.}$$

Here $\Delta\sigma$ is the cross section integrated over any fixed CM angular region with the invariant ratios $p_i \cdot p_j/s$ $(i \neq j)$ fixed. Allowing for the mass of the intermediate boson, these results can also be extended to weak interaction processes.

DERIVATION OF THE DIMENSIONAL SCALING LAWS [21]

Let us briefly discuss how the scaling laws for exclusive processes emerge from renormalizable quark field theories which are consistent with assumptions (A) and (B). First consider an n-particle scattering amplitude $\mathcal{M}_n$ obtained by replacing each hadron by a collection of quarks of the appropriate spin, with each constituent carrying a finite fraction of the hadron's momentum. (For example, n = 10 for meson-baryon scattering.) If we normalize spinors to $u^+u = 2E$, then $\mathcal{M}_n$ has dimensions [Length]$^{n-4}$.

In the case of Born approximation (i. e., the minimum non-loop connected diagrams), in renormalizable theories, we have the scaling $\mathcal{M}_n^{\text{Born}} \to [1/\sqrt{s}]^{n-4}$, in the asymptotic fixed angle limit. This follows directly from the fact that the coupling constant is dimensionless and the mass term can be neglected at large momentum transfer. (Note, though, that in the case of renormalizable Yang-Mills theories, this canonical scaling is only true for the total Born amplitude, and not necessarily for each diagram separately.)

We next consider the irreducible loop diagram contributions to $\mathcal{M}_n$, i. e.: those loop corrections to $\mathcal{M}_n^{\text{Born}}$ which will not be eventually summed by the Bethe-Salpeter wavefunctions. Because of Bjorken scaling and assumption (B) above, we must have $\mathcal{M}_n^{\text{Irred}} \to (\sqrt{s})^{4-n}$ [mod log s] in the scaling limit. We thus are assuming that the accumulation of logarithm from the higher order graphs will not affect the asymptotic scale invariance of the constituent interactions.

Finally, by definition, the complete hadronic amplitude is given by the convolution of the hadronic wavefunctions and $\mathcal{M}_n^{\text{irred}}$ integrated over the relative momenta $k_{(i)}^{\mu}$: [23]

$$\mathcal{M}_{\text{HAD}} = \int \psi_{\text{BS}} \psi_{\text{BS}} \mathcal{M}_n^{\text{irred}} \psi_{\text{BS}} \psi_{\text{BS}} \Pi d^4k_{(i)}. \tag{13}$$

Note that $\mathcal{M}_{\text{HAD}}$ can fall no faster than $\mathcal{M}_n^{\text{irred}}$. However, if

$$\int \psi_{\text{BS}}^{M}(k)\, d^4k \equiv \psi^{M}(x)\Big|_{x=0} < \infty \tag{14}$$

(and similarly for the baryons, integrating over both relative momenta) then the convergence of the d^4k integrations implies finite binding corrections, and

$$\mathcal{M}_{\text{HAD}} \to (\sqrt{s})^{4-n} \text{ [mod log s]} \tag{15}$$

in the fixed angle limit.

Although the finiteness of $\psi_{\text{BS}}(x)$ has not been proved in renormalizable field theories,[24] it is reasonable physically,[25] and follows if the Bethe-Salpeter kernel is slightly less singular at short distances than indicated

by perturbation theory (as well as in d < 4 dimensions). The above canonical scaling for $\mathcal{M}_{HAD}$ then gives the desired result,[21,22]

$$\frac{d\sigma}{dt} \to \frac{1}{s^{n-2}} f(t/s) , \quad [\text{mod} \log s] , \tag{16}$$

where n is the total number of external elementary fields (e, μ, γ, q, etc.), and the previous dimensional scaling laws follow.

The consistency of these exclusive scattering scaling laws with experiment indicates that the underlying degrees of freedom are given correctly by the quark field-theoretic models. Further experimental tests are crucial since the program is destroyed even if one scaling law is broken!

RESTRICTIONS ON THE MICROSCOPIC THEORY

The most natural candidates for a renormalizable spin $\frac{1}{2}$-quark field theory are the vector or scalar gluon theories. A particularly interesting possibility is that the assumed regular behavior of $\psi_{BS}(x)$ and canonical scaling of $\mathcal{M}_n^{irred}$ may be a property of the non-Abelian[26] "asymptotic freedom" gauge theories. However, any theory which allows the coupling of vector or scalar gluons has two serious conflicts with data: (1) the single gluon exchange diagram of Fig. 6a implies

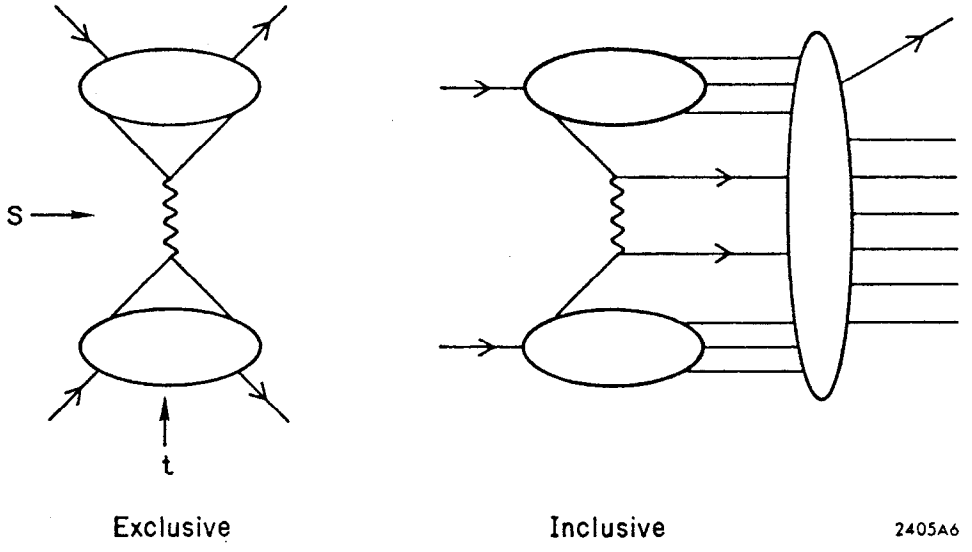

FIG. 6 — Direct elementary gluon exchange contributions to exclusive and inclusive hadron processes.

$$\frac{d\sigma}{dt} \to \underset{\text{(spin 1)}}{f(t)} \quad \text{or} \quad \underset{\text{(spin 0)}}{f(t)/s^2} \tag{17}$$

for $s \to \infty$, any fixed t. Both forms are in disagreement with the hadronic scattering data which show the effective trajectories decrease below $\alpha = 0$ at large t.[27] Multiple gluon exchange cannot appreciably change this s-dependence unless we assume an accumulation of logarithms, contrary to what is required from the dimensional scaling laws. (2) Furthermore, gluon exchange between the quark constituents of the incident hadrons yields a scale-invariant cross section for large transverse momentum inclusive hadron production, again contrary to experiment. In these processes the incident quarks scatter at large angles scale invariantly, and then by scale-invariant fragmentation produce the observed large transverse momentum hadrons [see Fig. 6b] .

Experimental evidence thus requires that gluon exchange between quarks of different hadrons is suppressed.[10,21] This could occur perhaps for dynamical reasons, because of the smallness of the coupling constants, or more interestingly, because of a selection rule. In fact, in theories with color symmetry[28], a colored gluon state — an octet in color SU(3) — cannot couple to hadrons, which are color singlets, and Fig. 6a would be absent. Further, if we assume that only color singlets appear in intermediate states, then multiple gluon exchange and Fig. 6b for inclusive processes would also be absent.[29]

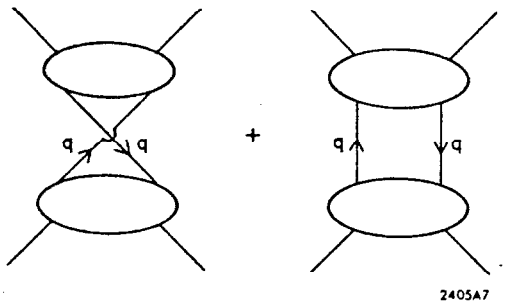

FIG. 7 — Quark interchange and quark interchange contributions to hadron-hadron scattering.

Independent of whether direct elementary gluon exchange takes place, constituent interchange inevitability takes place in any composite model.[10] Thus the quark-interchange and quark-exchange diagrams of Fig. 7 will always provide an interaction between the hadrons. Such diagrams are analogous to electron rearrangements in atom-atom collisions.

In fact for sufficiently large t and u, the interaction time becomes so brief that only these minimal quark interchange processes can occur.[10,30] Thus in the region of large momentum transfer the coherent Regge and multihadronic contributions are suppressed and the underlying constituent exchange mechanism can be exposed.

ASYMPTOTIC TRAJECTORIES IN THE INTERCHANGE MODEL[10,21]

Let us consider the quark interchange diagram of Fig. 8a in the "deep" Regge limit, $-u \to \infty$, with t fixed but large. Assuming the quark line carries a finite fraction x of the incident hadron B's momentum (we will justify below), then the upper part of Fig. 8a is determined from the

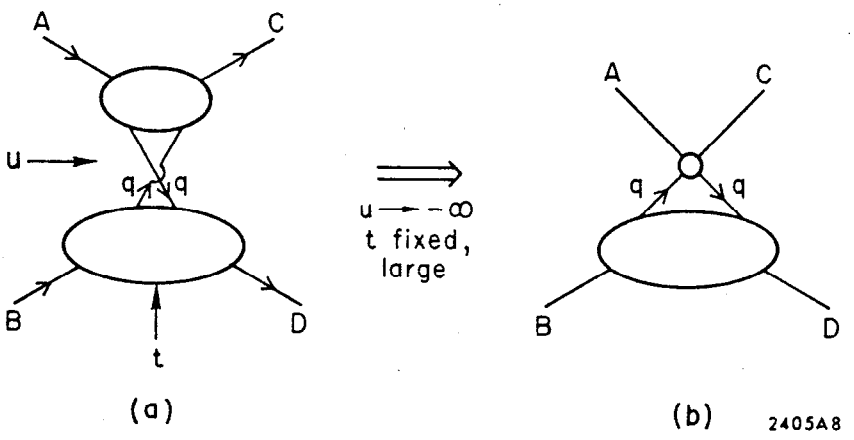

FIG. 8—Reduction of the interchange amplitude to a quasi-local form in the asymptotic Regge limit: $-u \to \infty$, fixed but large t.

large momentum transfer behavior of the amplitude $\mathcal{M}_{Aq \to Cq}$. Using the dimensional counting rules[21] we have

$$\mathcal{M}_{Aq \to Cq} \sim \begin{cases} 1/u \ (A, C = \text{mesons}) \\ 1/u^2 (A, C = \text{baryons}). \end{cases} \tag{18}$$

Diagram 8a thus collapses to an equivalent diagram 8b with an effective local $A + q \to C + q$ vertex behaving as inverse powers of u, and

$$\mathcal{M}_{A + B \to C + D} \to F_{BD}(t)(-u)^{\alpha_{AC}(t)} \tag{19}$$

where

$$\alpha_{AC}(t) \to \begin{cases} -1 & \text{Mesons} \\ -2 & \text{Baryons.} \end{cases} \qquad t \to -\infty$$

It is evident that the quantity $F_{BD}(t)$ is closely related to the electromagnetic form factor and has the identical asymptotic behavior. The resulting cross section for meson-baryon and baryon-baryon scattering thus have the form

$$\frac{d\sigma}{dt} \to \frac{1}{s^2} \frac{1}{u^{-2\alpha}} \frac{1}{t^4} \tag{20}$$

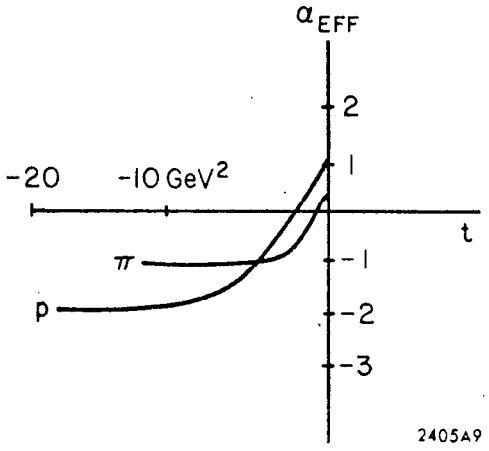

A recent fit to the effective trajectories in pp and πp elastic scattering by Blankenbecler, Gunion, Coon and Van Tran[27] is shown schematically in Fig. 9.

FIG. 9—Schematic representation of the effective trajectories obtained in the phenomenological analyses of Ref. 27 for $\pi p \to \pi p$ and $pp \to pp$ scattering. The uncertainties are of order $\pm\frac{1}{2}$ in α_{eff}.

Their results are consistent with the above predictions for α_{AC}, although the value for $\alpha(t)$ may be falling below -2 at the largest t values. These analyses take into account the signature factor dictated by the quark model.

In the case of Compton scattering at large t, $-u \to \infty$, the amplitude for the elementary $\gamma q \to \gamma q$ scattering at the top of the diagrams of Fig. 10 is energy-independent, corresponding to a δ_{J0} fixed singularity at $\alpha=0$.[31]

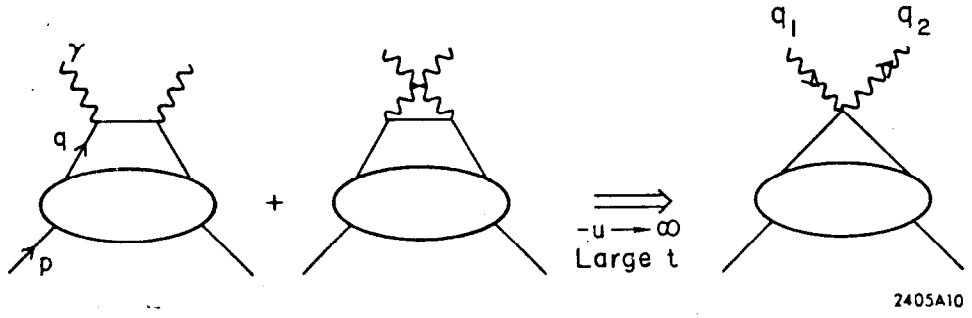

FIG. 10 — Reduction of the Compton amplitude to local J = 0 fixed pole behavior in the asymptotic Regge limit: $-u \to \infty$, large t.

Thus

$$\mathcal{M}_{\gamma p \to \gamma p} \to F_p^{(+)}(t)\, u^0\, \hat{\epsilon}' \cdot \hat{\epsilon} \tag{21}$$

and

$$\frac{d\sigma}{dt} \to \frac{1}{s^2}\,\frac{1}{t^4} \text{ for } s \to \infty,\ t \text{ large}. \tag{22}$$

The residue form factor $F_p^{(+)}(t)$ is similar to the e.m. form factor except that C = + states contribute in the t-channel. Not only is the amplitude energy independent, but also due to its local 2γ coupling, it is predicted to be independent of the photon masses q_1^2 and q_2^2 at fixed t.[31] This behavior can be checked in $e^{\pm} + p \to e^{\pm} + p + \gamma$ wide-angle bremsstrahlung measurements (the difference in cross sections yields the interference of the Compton and Bethe-Heitler amplitudes with one photon off shell), as well as in $\gamma + \gamma \to \pi^+\pi^-$ measurements possible via the two photon process in $e^{\pm} e^-$ colliding beams. A similar insensitivity to photon mass effects is also expected in the deep Regge fixed but large t limit in meson photoproduction: $"\gamma"p \to \pi p,\ \rho^0 p$, because the effective $\gamma q \to Mq$ amplitude becomes independent of the external masses at large u.[32]

CALCULATION OF THE ANGULAR DISTRIBUTION NEAR 90° [10,12]

The calculation of the full CM angular distribution of the "universal function" $f(\cos\theta_{CM}) = s^N d\sigma/dt$ of exclusive scattering beyond the form of the asymptotic trajectories requires some further assumptions. What we require in order to compute the quark interchange contribution to the

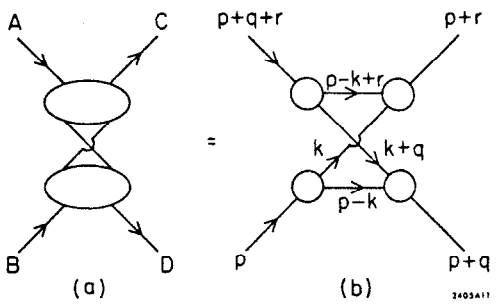

FIG. 11 — Interchange contribution to the hadronic amplitude at large t and u. In the case of meson-nucleon scattering, the line p - k represents two quarks or a "core" of the nucleon.

scattering A + C → B + D illustrated in Fig. 11a is the convolution of the amplitudes $\mathcal{M}(q + A \to q + C)$ and $\mathcal{M}(q + B \to q + D)$ at large t with off-shell parton legs. At large momentum transfer we can argue that the effects of the coherent multiparticle states which are associated with Regge phenomena and wee partons are absent, and these amplitudes are dominated by states with the least number of intermediate particles in the u channel.[10,30] The appropriate diagram at large t and u is thus Fig. 11b, where the vertices are given by the Bethe-Salpeter vertex functions.

With the labelling of the lines shown in Fig. 11b, we have $q^2 = t$ and $r^2 = u$. As an example, for $K^+p \to K^+p$ scattering the quark interchange model prediction would be that when $\mathcal{P}$-quark interchange is allowed, the line $p - k + r$ is a $\bar{\lambda}$ quark, and the line $p - k$ carries the quantum numbers of an $\mathcal{N} + \mathcal{P}$ quark state. Since the nucleon wavefunctions have the strongest off-shell behavior, the dominant contribution to the loop integrations comes from the region where $(p - k)^2$ is on the mass shell and either k^2 or $(k + q)^2$ is close to the mass shell. [In this case of $K^+p \to K^+p$ scattering, both contributions are identical.] We can then use the light cone, infinite momentum frame[10], or Sudakov variables[12] to parametrize $k^\mu \sim x p^\mu$ $(0 < x < 1)$, plus limited transverse momentum components.

Thus the large t and u behavior of the hadronic amplitude is dependent on the off-shell dependence of vertex function A with the lines $(p - k + r)^2 \sim xu$ and $(k + q)^2 \sim xt$ far off the mass shell, the vertex function C with the line $(p - k + r)^2$ off the mass shell, and the vertex function D with line $(k + q)^2$ off the mass shell. Accordingly, for large t and u[33]

$$\mathcal{M} \sim \int_0^1 dx\, P_B(x)\, \frac{\phi_D\big((1-x)t\big)}{(1-x)t}\, \frac{\phi_C(xu)}{xu}\, \phi_A\big(xu, (1-x)t\big)\,. \tag{23}$$

The factor $P_B(x)$ is obtained by integrating the non-asymptotic wavefunction of B over transverse momentum. Using the mean value theorem, we can also write this as

$$\mathcal{M}_{A+C \to B+D} \sim F_{BD}(t)\, \mathcal{M}_{q+C \to q+D}\Big|_{u' = \bar{x}u,\ t' = t} \tag{24}$$

Thus for $K^+p \to K^+p$ scattering, we have

$$\mathcal{M}_{q+K \to q+K} \sim \frac{1}{u'} \tag{25}$$

and

$$\frac{d\sigma}{dt} \sim \frac{1}{s^2}\,\frac{1}{t^4}\,\frac{1}{u^2} = \frac{1}{s^8}\,\frac{1}{(1-z)^4}\,\frac{1}{(1+z)^2} \tag{26}$$

and, by $s \leftrightarrow u$ crossing of the amplitude,

$$\frac{d\sigma}{dt}\,(K^- p \to K^- p) \sim \frac{1}{s^4 t^4} = \frac{1}{s^8}\,\frac{1}{(1-z)^4} \quad . \tag{27}$$

Thus the exotic exchange channel $K^+ p \to K^+ p$ is predicted to peak toward both the forward and backward directions, whereas $K^- p \to K^- p$, which has only the "box" (s,t planar) quark-exchange graph, only peaks in the forward direction (see Fig. 12). These expectations are born out by the data (see Fig. 3). Good agreement is also obtained for $\pi p \to \pi p$ elastic scattering which requires a linear combination of both the box and crossed graph contribution consistent with the quark interchange and anti-quark exchange contributions (see Fig. 13). Further, without any adjustments

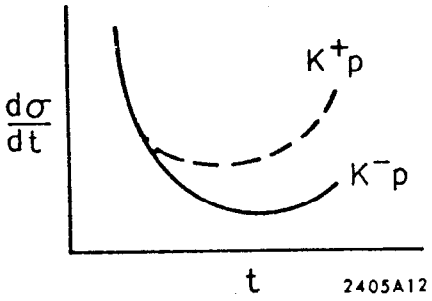

FIG. 12 — Schematic representation of the quark interchange prediction for the $K^{\pm} p \to K^{\pm} p$ angular dependence.

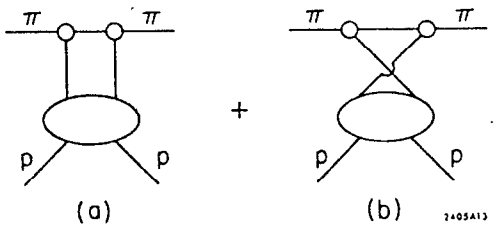

FIG. 13 — Quark exchange (st) and interchange (ut) contributions to $\pi - p$ scattering. The relative weighting of the two amplitudes can be determined from the quark model.

of normalization, $p\bar{p} \to \pi^+ \pi^-$ is predicted correctly simply by crossing the interchange amplitude (see Fig. 14). Further, more detailed calculations, including the effects of spin are given in Ref. 10.

The calculation of the angular distribution in the case of nucleon-nucleon scattering is much more model dependent. In Ref. 10, a two-particle quark + "core" bound state representation of the proton was used. The core was chosen to be dominantly spin 1 in order to reproduce G_E, G_M scaling, and the off-shell Bethe-Salpeter wavefunction was adjusted to give t^{-2} asymptotic behavior for the nucleon form factors. The result of a detailed calculation then gives

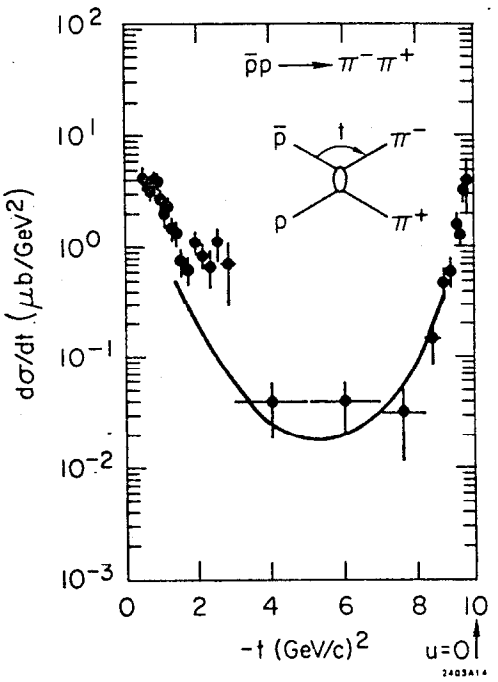

FIG. 14 — Prediction for the t-dependence of $p\bar{p} \rightarrow \pi^-\pi^+$ obtained from crossing the interchange amplitude normalized to $\pi p \rightarrow \pi p$ scattering. There are no free parameters. Data from CERN-Ecole Polytechnique-Orsay-Stockholm Collaboration.

$$\frac{d\sigma}{dt}(pp \rightarrow pp) \sim \frac{1}{s^{12}} \frac{1}{(1-z)^{5.2}}, \quad z \sim 0. \tag{28}$$

This angular distribution is not inconsistent with experiment (see Fig. 2) and yields via crossing

$$\frac{\frac{d\sigma}{dt}(p\bar{p} \rightarrow p\bar{p})\Big|_{90^\circ}}{\frac{d\sigma}{dt}(pp \rightarrow pp)\Big|_{90^\circ}} \sim \frac{1}{50}. \tag{29}$$

The experimental ratio is $\sim 10^{-2}$ (at $p_{lab} = 5$ GeV/c). [Note that the energy dependence s^{-12} in (28) disagrees with the dimensional scaling law prediction[21], s^{-10}, because a superrenormalizable binding interaction is required to produce t^{-2} behavior in the form factor using the two component model. Further fixed angle measurements of pp scattering at higher energies are thus very important in order to determine if the proton is described better at short distances as a parton plus core or a three quark field representation. Detailed calculation of the angular dependence in pp scattering using the three particle nucleon wavefunction has not yet been made.]

The model dependence of the pp scattering results illustrates a general point made by Fishbane and Muzinich[34] that the form factor (which only requires the dependence of the hadron wavefunction with one leg off shell) cannot uniquely determine the $pp \rightarrow pp$ scattering amplitude at large t and u (which requires a wavefunction with at least two legs off shell).

THE CONNECTION BETWEEN REGGE BEHAVIOR AND FIXED ANGLE SCATTERING[30]

In conventional treatments of Regge behavior, hadron scattering at large angles appears hopelessly complicated. One could never hope to unravel the effects of cuts, non-leading trajectories, and other secondary trajectories, and the other secondary singularities of the J-plane as they become increasingly important and intertwined as t and u become large. However, the simple nature of hadron scattering at large angles has led Blankenbecler, Gunion, Savit, and myself[30] to just the opposite conclusion: Regge behavior at large $|t|$ and $|u|$ is elegant and simple;

moreover, scattering in this region directly reflects the fundamental properties of the interacting hadrons at short distances.

The most dramatic implication for Regge theory is that all trajectories $\alpha_i(t)$ in hadron-hadron scattering will approach negative constants as $t \to -\infty$. [10,21]

Let us write the hadronic scattering amplitude in the form of an integral equation (see Fig. 15):

$$\mathcal{M} = K + K \otimes \mathcal{M} \, . \tag{30}$$

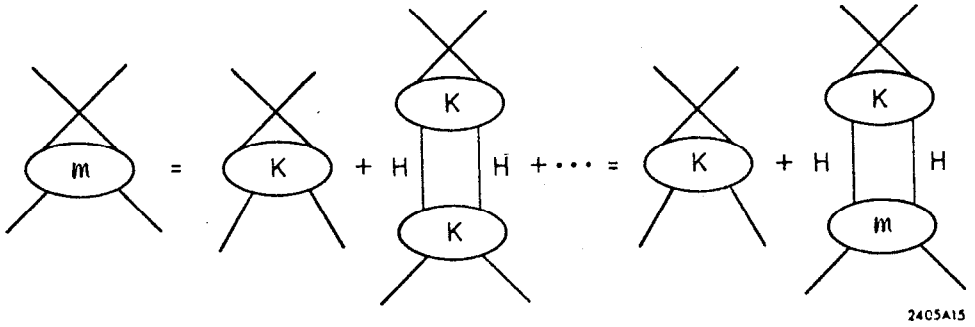

FIG. 15 — Integral equation for Hadron-Hadron scattering. The summation over H-H represents all two-particle hadronic states in the t channel.

The kernel K is by definition "hadron irreducible"; i. e. the last term contains all contributions from two-hadron states in the t channel. For large momentum transfer, we have $\mathcal{M} \to K$ since the multiple iterations of K fall rapidly in t. Thus we can identify K with the experimental amplitude at large angles. At small t, however, the iteractions of K in the t channel do contribute and produce moving Regge trajectories. The situation is very similar to the emergence of moving Regge trajectories in a ϕ^3 ladder series. The Born approximation $K \sim u^{-1}$ dominates at large t. At small t the iterations in the t channel give

$$\begin{aligned} \mathcal{M} &= \frac{1}{-u} + \frac{1}{-u} \log(-u)\, f(t) + \cdots \\ &\to (-u)^{\alpha(t)} \beta(t) \end{aligned} \tag{31}$$

where asymptotically

$$\alpha(t) = -1 + f(t) = \alpha(-\infty) + 0\,(t^{-1} \log t) \, , \tag{32}$$

and $\alpha(t)$ increases as $t \to 0^-$. When α comes close to the value + 1, s-channel iterations are important and must be included.

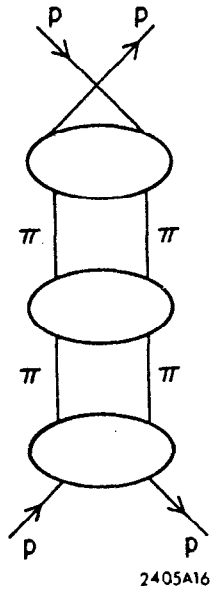

FIG. 16 — Example of the iteration of hadronic scattering amplitudes in a multi-channel model.

In the case of physical hadronic scattering, we need to consider a multichannel integral equation with kernels (which mix as in Fig. 16)

$$K_{MB \to MB'},\ K_{MM \to MM'},\ K_{BB \to BB}. \quad (33)$$

Because the kernels do not factorize, extra trajectories are produced. The result is shown in Fig. 17. There are two trajectories that become degenerate at $\alpha(t) = -1$ for $t \to -\infty$ which contribute to $\mathcal{M}_{MM \to MM}$ and $\mathcal{M}_{MB \to MB'}$, but cancel at large t in $\mathcal{M}_{BB \to BB}$. Another trajectory which goes to $\alpha(t) = -2$ or (-3) for $t \to -\infty$ couples to $\mathcal{M}_{BB \to BB}$. (The (-2) case corresponds to dimensional counting[21] and a three quark field representation; the (-3) case is for the parton + core representation of the proton.[10]) The first order variation of the trajectories away from their asymptotic values can be calculated in terms of the hadron form factors using the interchange model. Thus the forward and backward Regge amplitudes join smoothly onto the fixed angle behavior, and a beautiful synthesis of Regge dynamics with the underlying short distance behavior emerges. Further discussion may be found in Ref. 30.

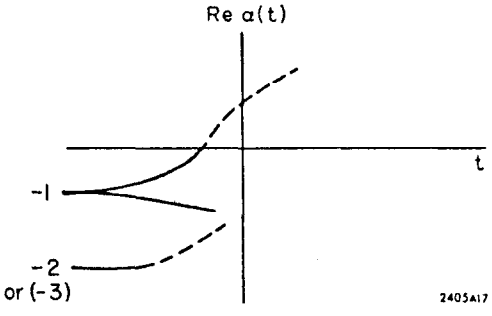

FIG. 17 —Effective Regge trajectories of meson-baryon and baryon-baryon trajectories, predicted from large angle behavior. From Ref. 30.

HADRONIC FEATURES OF PARTON MODELS[10,11,32]

As we have seen, a description of large transverse momentum interactions based on a simple, basic mechanism, such as quark interchange, will, by iteration of the hadronic scattering kernel K in the t or u channels, join on smoothly to a Regge description of low momentum transfer events. The parton or quark field-theoretic model of composite hadrons can thus lead to an elegant, unified description of hadron dynamics based on a very few degrees of freedom.

This interplay of parton and hadron intermediate states also leads to an understanding of some heretofore confusing aspects of the parton model, such as how the hadronic interactions are propagated over long distances if parton effects are confined to short range, how the hadron-like vector dominance features of photon interactions emerge, and what is the range of validity of the impulse approximation in hadronic and electromagnetic interactions.[32]

The key to unravelling the basic parton processes from the complicated hadronic effects is to distinguish the two component nature of the composite hadron's wavefunction. Consider deep inelastic electron-proton scattering in a frame in which the proton is incident with a large momentum P. We can identify two different contributions to the deep inelastic process. In the "hadron reducible" contribution shown in Fig. 18a, the photon interacts with a quark current which is actually the constituent of a secondary hadron H bremsstrahlunged from the proton. In the "irreducible" contribution, the struck quark-parton originates directly from the proton (see Fig. 18b). Because the $\overline{H}$-p cross section has Regge behavior:

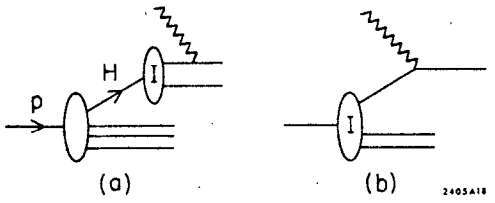

FIG. 18 — Contributions to the hadron-reducible and hadron-irreducible components of the proton wavefunction to deep inelastic lepton scattering. The reducible component contains the wee quark and Regge contributions.

$$\sigma_{\overline{H}p} \sim s^{\alpha-1} \quad (\alpha \sim 1) \ , \tag{34}$$

it is easy to show that the spectrum of fractional longitudinal momentum z of hadron H in the proton has the Feynman form dz/z^{α}, for $z \sim 0$, and the resulting Bjorken-scaling structure function is Regge behaved:[35] $F_2(\omega) \sim \omega^{\alpha-1}$ for $\omega \to \infty$. Thus the so-called "wee" parton spectrum can be identified with the quark constituents of the hadronic bermsstrahlung products emitted by the incident hadron. In the rest frame, the wees are the quark constituents of the hadrons in the periphery of the target. The propagation of the hadronic interactions over large distances then occurs via these hadronic intermediate states. The quark propagation only needs to occur over a short range within the interior of the interacting hadrons.

In contrast to the Regge-hadronic bremsstrahlung contributions, the irreducible wavefunction can be identified with a Bethe-Salpeter amplitude involving only the minimum number of constituent fields; accordingly, its contribution to $F_2(\omega)$ vanishes as a power for $\omega \to \infty$. Similarly, in the threshold region, $\omega \equiv x^{-1} \sim 1$, the irreducible component contribution vanishes as $F_2^I(\omega) \sim (1-\omega)^p$, as required by the off-shell behavior of the Bethe-Salpeter wavefunction. (The reducible vanishes even more rapidly at threshold because of the extra suppression at $z > 1/\omega \sim 1$.)

In the case of the elastic proton form factor, the hadron-reducible wavefunction contribution (Fig. 19a) clearly vanishes rapidly at large t due to the rapid decrease of the H-p scattering amplitude. The irreducible, Bethe-Salpeter component (Fig. 19b) gives a power-law fall-off $F(t) \sim t^{-\frac{1}{2}(1+p)}$ related to the behavior of $F_2(\omega)$ at $\omega \sim 1$. The Drell-Yan relation, and simple crossing behavior[36] to the timelike channel for F(t) at large t and $F_2(\omega)$ for $\omega \sim 1$ thus emerges because of the dominance of simple hadron-irreducible contributions in these regions.

The physics of the Compton amplitude $\gamma p \to \gamma p$ also becomes clarified when we take into account the hadronic bremsstrahlung contribution. Consider scattering at low t first. The Regge contribution to the H-p scattering amplitude of Fig. 20a implies that it is the hadrons, and hence

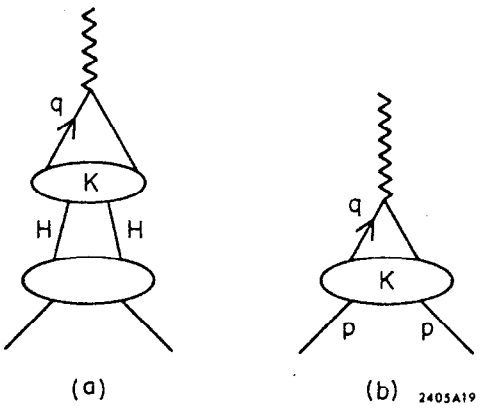

FIG. 19 — Contributions of the hadron-reducible and hadron-irreducible scattering amplitudes to the elastic form factor.

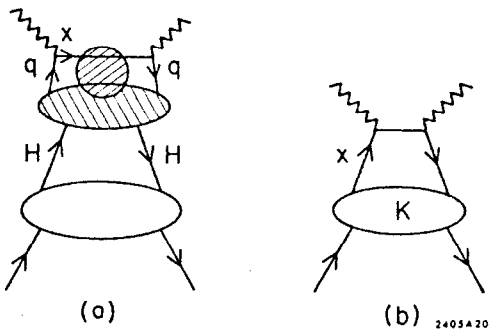

FIG. 20 — Contributions of the hadron-reducible and hadron-irreducible scattering amplitude to the Compton amplitude.

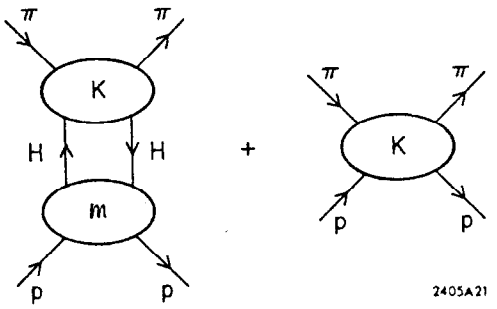

FIG. 21 — Contributions of the hadron reducible and irreducible kernel components to exclusive hadron scattering.

quarks, with an arbitrarily small fraction of the proton's momentum which interact with the photon. The effective γ-q collision energy is thus

$$\nu_{\text{eff}} = \langle x \rangle \nu \qquad (35)$$

with $\langle x \rangle \sim 0(1/\nu)$. There is clearly no impulse approximation involved here; arbitrary number of hadronic interactions are allowed along the struck parton line and we can expect binding corrections similar to those implied by vector meson dominance to arise. Further, the variable change $x = \bar{x}/\nu$, which gives the dominant region of the parton longitudinal momentum integration, implies that the Compton amplitude has the same Regge behavior as the hadronic amplitude. However at large t, the leading trajectories recede, the Hp $\rightarrow$ Hp amplitude is suppressed and the irreducible amplitude shown in Fig. 20b survives. Since the hadronic trajectories are below $\alpha = 0$, we have $\nu_{\text{eff}} \equiv \langle x \rangle \nu \rightarrow \infty$, for $\nu \rightarrow \infty$, and the elementary local J = 0 fixed pole behavior of the $\gamma q \rightarrow \gamma q$ amplitude dominates. Thus large t does imply impulse approximation for the Compton amplitude! Additionally, even at small t, if the photon line is virtual $[k_1^2 \sim 0(\nu)]$ then the parton line again carries large momentum and a scaling result at fixed ν/k_1^2 emerges.[32] Similar results also apply to meson photoproduction and electroproduction.[37]

Coming back full circle to hadron-hadron scattering, it is clear that the hadron-irreducible components dominate at large u and t and can be calculated from the simplest irreducible kernels K (see Fig. 21b). If we identify K with the quark interchange or exchange graphs, then a simple dynamical interpretation of the Harari-Rosner duality diagrams can be made. At large t and u only the skeleton duality diagram displaying the minimum number of quark lines needs to be

FIG. 22 — Calculation of a duality diagram at large momentum transfer. The bubbles represent the meson Bethe-Salpeter wavefunctions.

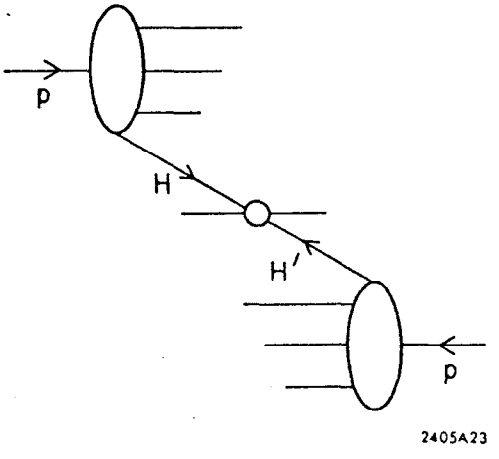

FIG. 23 — Typical inclusive reaction at small transverse momentum. The collision of the hadrons H and H' occurs at low energy.

considered, and it may be calculated using the minimal Bethe-Salpeter bound state representations of the hadrons as indicated in Fig. 22. At small t or u, diagrams of the type shown in Fig. 21a dominate. In this case π-p scattering proceeds dominately via low energy π-H collisions. It is easy to check that these reducible contributions from the iteration of K in the t or u channel correspond to loop insertions in the basic duality diagram structure.

In the case of typical inclusive collisions involving low momentum transfer, the irreducible interaction typically involves the low energy collision of two bremsstrahlung components H and H' of the incident particles (see Fig. 23). This picture is very much like the multiperipheral model: most of the beam energy is lost down the beam directions (in the CM) so that the irreducible collision (whose cross section decreases rapidly with energy) occurs at the smallest possible s_{eff}. A slow, logarithmic dependence on the initial s is thus to be expected. Thus if we wish to probe the fundamental interactions at large energies, in order to see small distance effects, we must rely on large transverse momentum production processes. The effective energy that matters is not s, but rather

$$s_{eff} = 4p_\perp^2 \qquad (36)$$

where $p_\perp$ is the total transverse momentum produced on one side of the reaction.

INCLUSIVE PROCESSES AT LARGE TRANSVERSE MOMENTUM[21,12]

The scaling behavior of the inclusive cross section $d\sigma/(d^3p/E)$ $(A + B \to C + X)$ at fixed invariant ratios is crucially sensitive to the scaling properties of the basic hadronic interactions at short distances. Thus, as we have discussed, if the dominant mechanism for transferring large transverse momentum is a scale-invariant quark-quark interaction between quarks of the incident hadrons, then — because fragmentation probabilities of hadrons into quarks (and vice-versa) are also scale invariant — $d\sigma/(d^3p/E) \sim p_\perp^{-4}$ at fixed $p_{CM}/\sqrt{s}$ and θ_{CM}, just on dimensional grounds alone.[9]

Whether or not such quark-quark interactions are important (they of course always occur on the electromagnetic level), we can never preclude basic interactions of the type[11,12] $q + M \to q + M$, $q + \bar{q} \to M + \bar{M}$, or even[38] $q + q \to B + \bar{q}$, which must occur, simply by the existence of the bound state wavefunctions and constituent interchange. In each of the above cases, six elementary fields are involved in the large momentum transfer reaction, and by dimensional counting (or the interchange model in the case of the quark-meson reactions) the two-body cross sections scale as $d\sigma/dt \sim s^{-4}$ compared to s^{-2} for scale-invariant four-field interactions. Accordingly we have at fixed $p_{CM}/\sqrt{s}$, θ_{CM} [21]

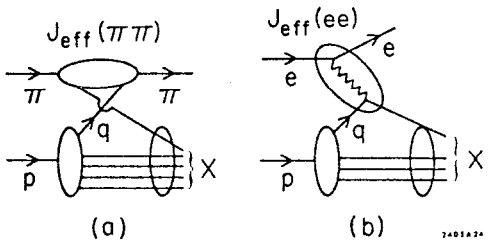

FIG. 24 – Comparison of deep-inelastic hadron scattering $\pi p \to \pi X$ and deep inelastic lepton scattering $ep \to eX$. The hadronic reaction is controlled by the elementary amplitude for $\pi q \to \pi q$ scattering.

$$\frac{d\sigma}{d^3p/E} \sim \begin{cases} \frac{1}{p_\perp^8} & \pi p \to \pi X,\ pp \to \pi X,\ pp \to pX \\ \frac{\alpha}{p_\perp^6} & \gamma p \to \pi X,\ \pi p \to \gamma X \\ \frac{\alpha^2}{p_\perp^4} & \gamma p \to \gamma X,\ ep \to eX,\ pp \to \mu X\,. \end{cases} \tag{37}$$

Note that the order α cross sections can utilize the reactions $\gamma q \to q\pi$. In the case of proton production, if $qq \to p\bar{q}$ were suppressed, the interchange mechanism $qp \to qp$ which gives $p_\perp^{-12}$, would be important. The calculations of the detailed cross sections are simple using the interchange model.[11] We begin with $\pi p \to \pi X$, and for the moment ignore the complications of hadronic radiation or bremsstrahlung from the meson lines. If we compare Fig. 24a for hadron scattering with Fig. 24b for $ep \to eX$, then one can write immediately

$$\frac{d\sigma}{dtdx}(\pi + p \to \pi + X) = \frac{F_{2p}(x)}{x}\,\frac{d\sigma}{dt}(q + \pi \to q + \pi)_{p_a = xp}\,. \tag{38}$$

where $x = \omega^{-1} = -t/(\mathcal{M}^2 - t)$ is the Bjorken variable. The required differential cross section for quark-meson scattering is to be evaluated for on-shell quarks, where the incident quark has a fraction x of the proton's momentum (in a frame where the proton has arbitrary large momentum). Thus $s' = xs$, $u' = xu$, and $t' = t$ in the elementary subprocesses. The effective current J(ee) for $e + q \to e + q$ (via photon exchange) in deep inelastic electron scattering is replaced by the effective current $J(\pi\pi) = O(1/xu \pm 1/xs)$ for $q + \pi \to q + \pi$ in deep inelastic pion scattering. In the case of $\pi p \to KX$, the effective current $J(\pi K)$ is strangeness changing.

The above calculation is somewhat oversimplified since hadronic radiation — or bremsstrahlung — from the incident and final external lines must also be taken into account, much like the electromagnetic radiative corrections in deep inelastic lepton scattering. When $2p_{CM}/\sqrt{s}$ is not near its kinematic limit of 1, then it is probable that the incident hadrons will radiate as much energy as possible so that the elementary quark-hadron

interaction takes place at the minimum possible energy. However, because these fragmentation functions are scale invariant, none of the inclusive scaling laws change!

As an example, consider the process $pp \to \pi X$. The large transverse momentum reaction is $q + M \to q + \pi$ where M is a meson which is a bremsstrahlung component of the upper proton in Fig. 25 and π is the detected hadron. Let $G_{H/p}(z)$ be the probability distribution for hadron H

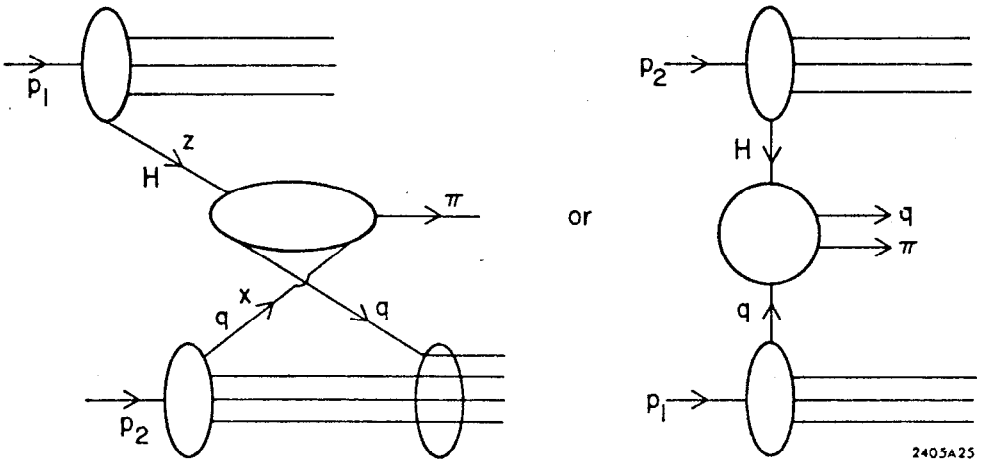

FIG. 25 — The inclusive process $pp \to \pi X$ at large transverse momentum. The elementary subprocess which produces $p_\perp^{-8}$ behavior is $H + q \to \pi + q$ where H is produced by fragmentation (hadronic bremsstrahlung). In (b) the same process is displayed in the form of a multiperipheral chain.

to have a fraction z of the proton's longitudinal momentum (in the proton's infinite momentum frame). A reasonable form for G is

$$G_{H/p}(z) \sim \frac{(1-z)^{n_H}}{z^{\alpha}} \tag{39}$$

where the behavior at $z \sim 0$ reflects the behavior of the asymptotic $\sigma_{\bar{H}p} \sim s^{\alpha-1}$ cross section ($\alpha \sim 1$). [A reasonable guess for n_H might be $n_H \sim 4$ or 5, although this is model dependent.] Then we have

$$\frac{d\sigma}{dtdx}(pp \to \pi X) = \sum_H \int_0^1 dx\, G_{H/p}(z)\, \frac{d\sigma}{dtdx}(H + p_2 \to \pi + X)\Big|_{p_H = zp_1} . \tag{40}$$

The required $H + p \to \pi + X$ cross section is irreducible with respect to the hadron line H, but contains, by the definition of $F_{2p}(x)$, the full contribution of the lower proton line. It is evaluated at $\bar{s} = zs$, $\bar{u} = u$, $\bar{t} = zt$.

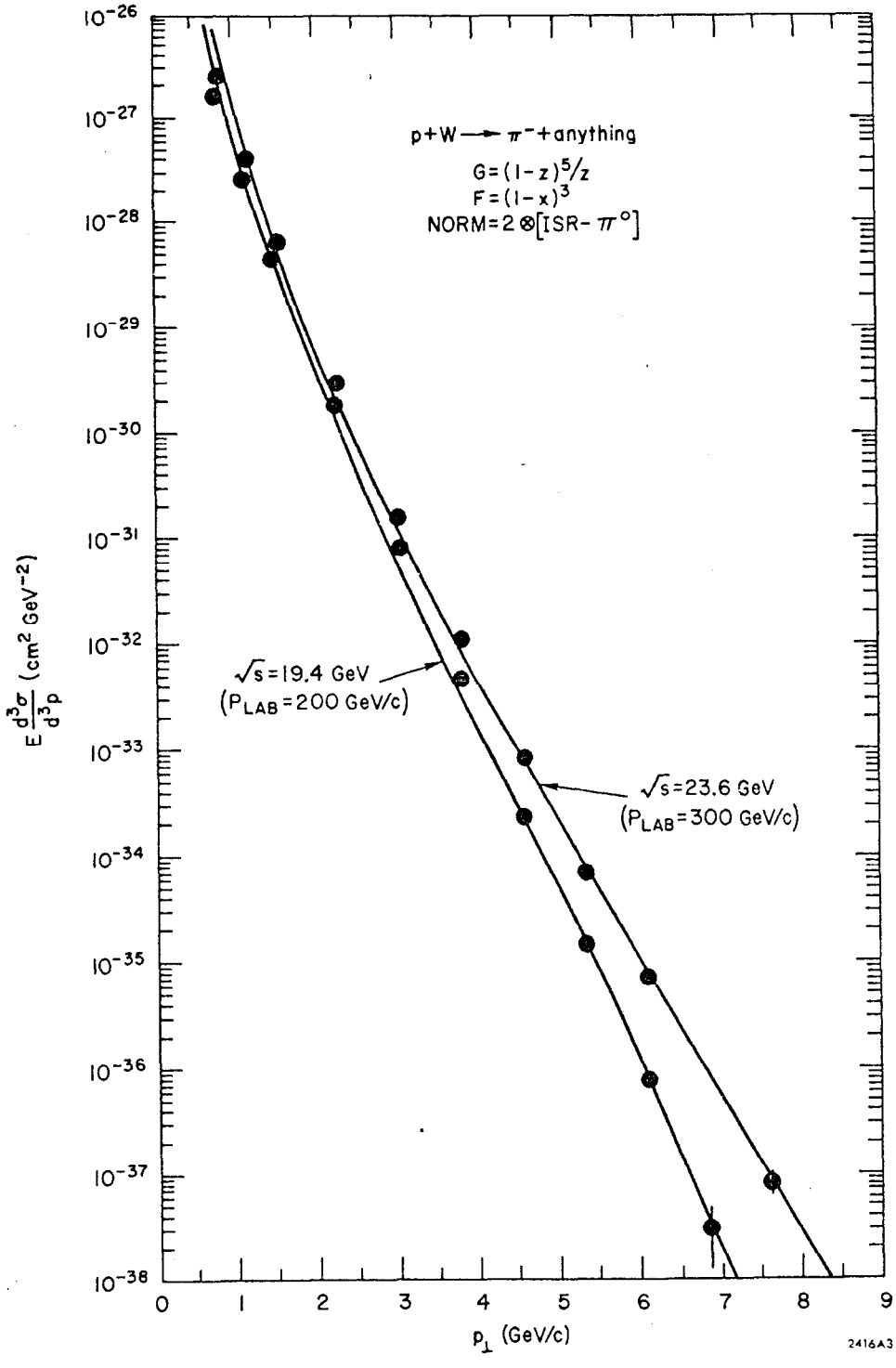

FIG. 26 — The prediction of the interchange model for $pp \rightarrow \pi^- X$, compared with the NAL data of Ref. 4. An overall factor of 2 change in normalization is assumed relative to the data of Ref. 1.

This result again gives $d\sigma/(d^3p/E) \sim p_\perp^{-8}$ at fixed $p_\perp/\sqrt{s}$, $p_L/\sqrt{s}$ in agreement with experiment.[1] (See Fig. 1.) A detailed comparison with the ISR[1] and NAL[4] cross sections is shown in Figs. 26 and 27, assuming $G_{H/p} = (1-z)^5/z$. An overall factor of 2 renormalization of the NAL data relative to the ISR data was used.[39]

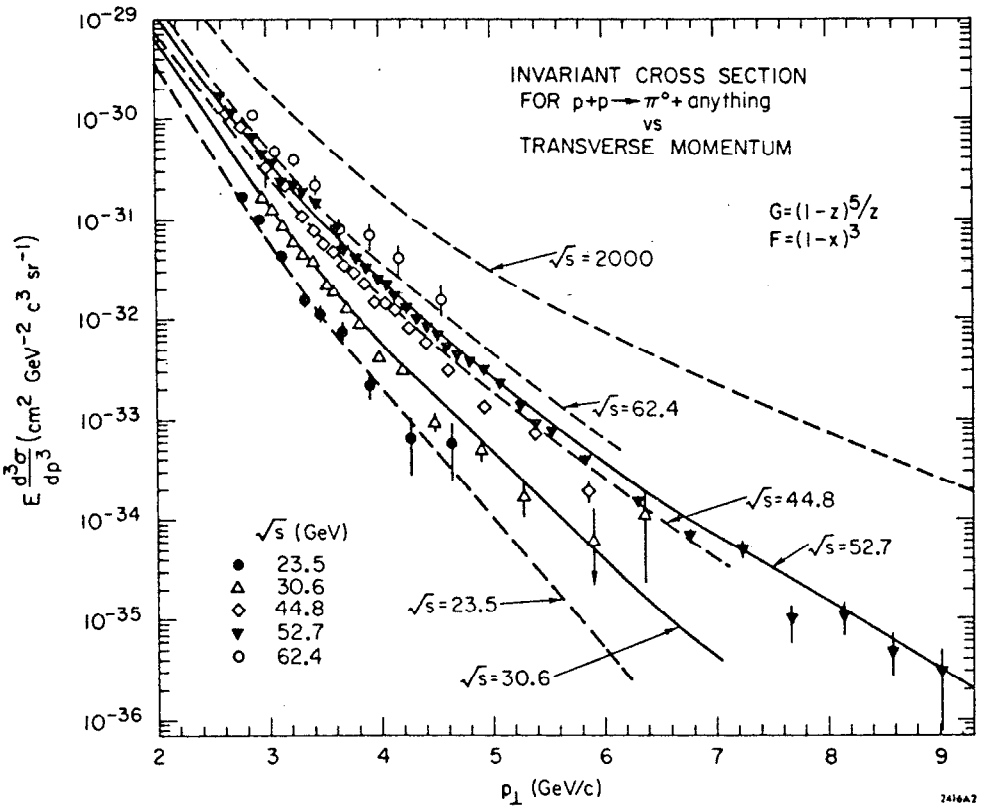

FIG. 27 — The prediction of the interchange model for $pp \to \pi^0 X$, compared with the ISR data of Ref. 1.

Because of hadronic bremsstrahlung, the overall picture somewhat resembles a multiperipheral picture as shown in Fig. 25b.[40] As we have shown elsewhere,[11] the inclusive cross section in the interchange theory has the form of the standard fragmentation, triple-Regge and pionization formulae in their respective regions, but in addition predicts the effective residues and trajectories at large t or $p_\perp^2$ in consistency with the results found for the exclusive scattering at large t and u.

The behavior of the inclusive cross sections at fixed θ_{CM} over the full range of transverse momentum is indicated schematically in Fig. 28:

For $p_\perp \ll \sqrt{s}$, the cross section becomes independent of energy and thus obeys Feynman scaling. In the region where $p_\perp \ll \sqrt{s}$, but $p_\perp$ large compared to typical hadronic masses, we have $d\sigma/(d^3p/E) \sim p_\perp^{-8}$, which agrees with the British-Scandinavian results at the ISR.[3] For very

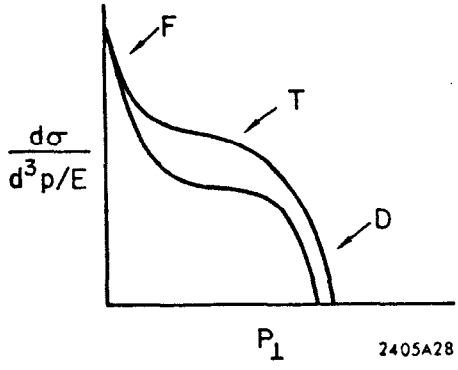

FIG. 28 — The qualitative features of the invariant cross section for two different energies as a function of $p_\perp$ (at fixed θ_{CM}) predicted by the interchange model.[11] The regions F, T, and D refer to the Feynman scaling, transition, and deep scattering regions, respectively.

large $p_\perp$, i.e.: $2p_{CM}/\sqrt{s}$ approaching its kinematical limit, only the hadron-irreducible components survive, and many restrictions due to quark counting (e.g. absence of antiquarks for $x \sim 1$ in the proton wavefunction) and connections to exclusive processes become controlling. Between this "deep scaling" and the Feynman scaling regions is the "transition" zone where the hadronic bremsstrahlung processes partially Reggeize the cross section, giving cross sections of the form of an inverse power of $p_\perp$ times a decreasing function of the ratio $p_{CM}/\sqrt{s}$.

THE FINAL STATE IN DEEP-INELASTIC HADRON REACTIONS[41]

Predictions for the composition and nature of the final state in inclusive reactions are always more treacherous than predictions for scaling laws in parton models since the mechanism for containing the single particle quark and elementary gluon states is unknown. We can only assume that there is some long-range interaction (which does not disturb the power laws) that operates to recombine the quark or color quantum numbers in e^+e^- annihilation, deep inelastic lepton-hadron scattering, and deep inelastic large transverse momentum inclusive hadronic reactions.

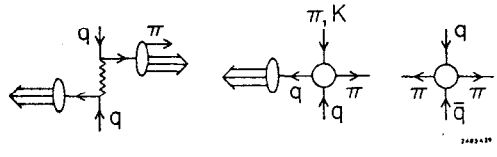

FIG. 29 — Elementary subprocesses for meson production at large transverse momentum. (a) Elementary quark-quark scattering via gluon exchange,[9] (b) quark-meson scattering,[11] (c) $q\bar{q} \to \pi\pi$.[12]

Let us consider the production of large transverse momentum hadrons in a pp collision as viewed from the CM frame. The elementary subprocesses which can contribute are illustrated in Figs. 29 and 30. In each case the incident proton beams fragment into quark or meson components which collide along the beam (North-South) direction. In the case of the gluon exchange reaction of Fig. 29a the quarks scatter at large angles and fragment to produce a "double jet" final hadronic state similar to that expected in e^+e^- annihilation. Note, however, that because of the spectrum of momentum of the incident initiating particles, the center of mass of the qq system is generally not at rest

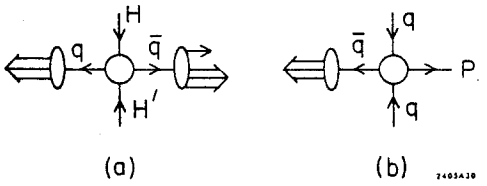

FIG. 30 — (a) The elementary subprocesses meson + meson → q + q̄ leading to a two-jet hadronic final state. (b) The elementary subprocesses q + q → p + q̄ which can be important for pp → pX reactions. The cross sections $d\sigma/(d^3p/E)$ illustrated in Figs. 29b, c and 30a, b scale as $p_\perp^{-8}$ at fixed $p_\perp/\sqrt{s}$, θ_{CM}.

relative to the proton-proton system. Thus a leading large $p_\perp$ hadron detected at 90° generally has its momentum balanced by a hadronic system with a sizeable longitudinal component.

Because of the observed power law behavior, the $p_\perp^{-8}$ reactions of Fig. 29b, 29c, and 30 are apparently dominant as we have discussed in the previous section. These also can give double jet fixed states, but various subprocesses are favored for a given final state. In particular, the reaction pp → πX with only one meson tagged at large transverse momentum may be dominated by the subprocesses 29b or 29c since these allow the minimum effective energy $s_{eff} \cong 4p_\perp^2$. In contrast, the double-quark subprocesses 30a with subsequent fragmentation of a quark into the pion involves a larger s_{eff} since the quarks are produced with extra transverse momentum. Reaction 29c is probably dominant for double-inclusive processes pp → ππX where two mesons are measured at opposite high $p_\perp$. The reaction 30b allows direct production of a high $p_\perp$ nucleon with a quark jet on the opposite side. The analogous process $\bar{q}\bar{q} \to \bar{p}q$ is presumably doubly suppressed at large $p_\perp$ due to the suppression of antiquarks with a large fraction of the incident proton's momentum. All of these $p_\perp^{-8}$ processes can be important in double jet measurements or experiments which only require the production of a large total transverse momentum.[42]

The final state in deep inelastic hadron processes like pp → πX shares some features of deep inelastic electron scattering ep → eX when radiation effects are taken into account (see Fig. 31). In the leptonic case the incident lepton emits a spectrum of soft and hard photons which will lower the effective energy of the high momentum transfer subprocesses. There is also (dominantly soft) photon radiation along the direction of the detected lepton associated with the reconstruction of the self-field of the physical particle.

Similarly in pp → πX hadronic bremsstrahlung (i. e. fragmentation) along the beam line is probable since it lowers the effective energy of the large momentum subprocesses. If the subprocess πq → πq is involved, then at least one nucleon would be included in the beam fragments. Also, as in deep inelastic electron scattering, we expect soft radiation to be emitted along the detected hadron direction in order to construct the self-field of physical hadron.[43] This hadronic radiation is limited, however, because it raises the s_{eff} of the subprocess. The composition of the state X_0 parallels the inclusive missing mass hadronic state in deep inelastic e-p scattering.

It is certain that future experiments which study

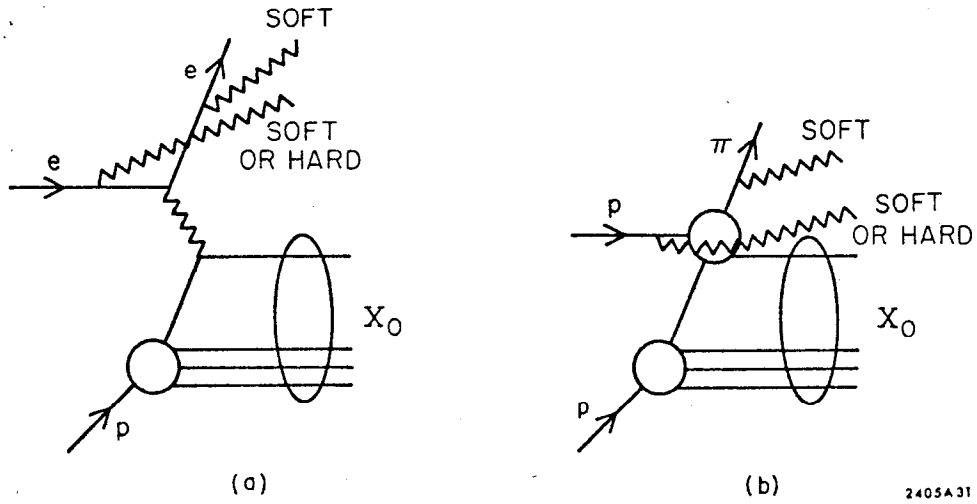

FIG. 31 — Comparison of final states in $ep \to eX_0$ (plus electromagnetic bremsstrahlung) with $pp \to \pi X_0$ (plus hadronic bremsstrahlung).

(a) the complete range of $p_\perp$ and p_L up to their kinematical limits,
(b) π, K, $\bar{p}$, and γ - initiated reactions, and
(c) possible jet structure and other dynamical features.

will be extremely interesting. In particular with the beams listed in (b), the antiquark and strange quark suppression at large s_{eff} is removed and a detailed analysis of the important high momentum subprocesses can be made.

CONCLUSIONS

It is clear that exclusive and inclusive processes at large transverse momenta are probing the dynamics and fundamental properties of hadrons at short distances. Although we await much more experimental information, the following conclusions are beginning to emerge:

1. The scaling laws of large transverse momentum exclusive processes, along with Bjorken scaling, strongly indicate a composite representation of the hadrons based on quark-field degrees of freedom.[21] Miraculously, the simplest possible dimensional analyses works! The scaling laws are consistent with finite Bethe-Salpeter hadronic wavefunctions and scale-invariant quark-quark interactions within the hadrons.

2. The $p_\perp^{-8}$ scaling behavior of the deep-inelastic hadron cross section[1] (at fixed $p_{CM}/\sqrt{s}$ and θ_{CM}) and the angular distributions of the exculsive processes[10] at large u and t demand the suppression of scale-invariant (single or multiple) gluon exchange interactions between quarks of different hadrons.[44] This may point to a strong selection rule forbidding the emission of color states from color-singlet hadronic states,[29] although possibly it is a result of dynamics (e.g. heavy color states) or a small effective coupling constant.

3. The canonical nature of the scaling laws — indicating the absence of effects due to the accumulation of logarithms from the loop corrections in renormalizable field theories — may be evidence pointing toward non-Abelian "asymptotic freedom" gauge theories.[26] The derivation of the scaling laws shows that the short distance properties of the hadron play an essential role at large momentum transfer even when all the external lines are on-shell.[21, 45]

4. We have found that Regge theory is extremely elegant and simple at large momentum transfer: all the trajectories are predicted to approach negative integers at large t with the residue functions $\beta(t)$ behaving similar to the elastic form factors.[11,32] These new results imply a broad spectrum of new constraints on the phenomenology and dual behavior of hadronic reactions.[46]

5. At large momentum transfer the multihadronic and "wee" components of the hadron wavefunction become suppressed and a Bethe-Salpeter description of its hadron-irreducible structure based on a minimal quark field representation emerges.[33] Thus only the "valence" quarks are important at $x \sim 1$ or large $p_\perp$ and simple inverse-power law behavior in the off-shell variables is expected. This implies the absence of leading Regge multihadronic effects in exclusive processes at large t and u, and the scattering becomes dependent on the simplest basic processes at short distances. Assuming these processes are quark interchange and quark exchange, the resulting scattering amplitude at large t and u is a dynamical realization of the simplest non-loop duality diagrams.

6. Striking differences between vector mesons and on-shell photon interactions must occur in large transverse momentum reactions if the elementary constituent basis of hadrons is valid. Examples of this are the unique scaling laws predicted for photon reactions [e.g. $p_\perp^{-6}$ behavior for $d\sigma/(d^3p/E)\,(pp \to \gamma X)$] and the local q^2- independent two-photon $J=0$ fixed pole behavior of the Compton amplitude at large t.

7. The apparent success of scaling laws based on the dynamics of quasi-free quarks within the hadrons now compounds the mystery of why free quarks or gluon states do not appear. Hopefully, the new clues gained from the large transverse momentum reactions—especially the evidence for the absence of gluon exchange between the constituents of different hadrons—will help point the way to a solution of this central problem. Physically, one can argue from potential theory that closely-packed bound state levels are well approximated by a free continuum state.[47] Accordingly, since quarks are not observed, a "dual" representation of all the literal quark results in terms of an equivalent summation over hadron states must be possible.[48,49]

ACKNOWLEDGEMENTS

I would like to thank J. Bjorken, R. Blankenbecler, G. Farrar, J. Gunion, G. Preparata, and R. Savit for many helpful discussions. I would also like to thank Dr. R. Peierls for the hospitality of the theoretical physics group at Brookhaven National Laboratory where this talk was prepared.

REFERENCES

1. CERN-Columbia-Rockefeller Collaboration, paper submitted to the XVI International Conference on High Energy Physics, Chicago-NAL (1972). F. W. Busser et al., CERN preprint, August 1973 (submitted to Physics Letters).
2. Saclay-Strasbourg Collaboration, paper submitted to the XVI International Conference on High Energy Physics, Chicago-NAL (1972). M. Banner et al., Phys. Letters 44B, 537 (1973).
3. British-Scandinavian Collaboration, paper submitted to the XVI International Conference on High Energy Physics, Chicago-NAL (1972); B. Alber et al., Phys. Letters 44B, 521, 527 (1973).
4. J. Cronin et al., presented to the II Aix-en-Provence International Conference on Elementary Particles, September (1973).
5. J. D. Bjorken, Proceedings of the 1967 International Conference on Electron and Photon Interactions at High Energies, SLAC (1967). R. P. Feynman, Phys. Rev. Letters 23, 1415 (1969). J. D. Bjorken and E. A. Paschos, Phys. Rev. 185, 1975 (1969).
6. For a recent review of the data and evidence for scaling, see E. Bloom, presented to the International Symposium on Electron and Photon Interactions at High Energies, Bonn, August (1973).
7. Including systematic uncertainties N has a total error of ± 0.70.
8. S. Berman and M. Jacob, Phys. Rev. Letters 25, 1683 (1970).
9. S. Berman, J. Bjorken, and J. Kogut, Phys. Rev. D4, 2381 (1971). See also D. Horn and F. Moshe, Nucl. Phys. 48B, 557 (1972), D. Cline, F. Halzen, and M. Waldrop, University of Wisconsin preprint (1973), S. Ellis and M. Kislinger, NAL preprint (1973). A. Casher, S. Nussinov, and L. Susskind, Tel-Aviv University preprint (1973).
10. The applications of the interchange model to exclusive processes are given in R. Blankenbecler, S. Brodsky, and J. Gunion, Phys. Letters 39B, 649 (1972), and Phys. Rev. D8, 287 (1973).
11. The applications of the interchange model to inclusive processes are given in R. Blankenbecler, S. Brodsky, and J. Gunion, Phys. Rev. D6, 2652 (1972), and Phys. Letters 42B, 461 (1972). The first paper discusses deep inelastic hadron scattering where hadronic bremsstrahlung processes can be suppressed. The general predictions are given in the second reference.
12. A covariant formulation of the interchange model in a less specific framework than Ref. 11 is given by P. V. Landshoff and J. D. Polkinghorne, Phys. Rev. D8, 1972 (1973), and J. C. Polkinghorne, report to the II Aix-en-Provence International Conference on Elementary Particles, September (1973).
13. A multiperipheral model based on treating mesons as elementary fields in a ϕ^3 model is given by D. Amati, L. Caneschi, M. Testa, Phys. Letters B43, 186 (1973). Because of its superrenormalizable nature, this model gives N = 8 in Eq. (4).
14. C. Baglin et al., CERN preprints (1973), submitted to Phys. Letters. A review of the large-angle data is given by A. Lundby, this conference.

15. P. V. Landshoff and J. C. Polkinghorne, Cambridge report No. DAMTP 73/4 (unpublished). See also Fig. 8 of Ref. 10.
16. D. P. Owen et al., Phys. Rev. 181, 1794 (1969). These results are consistent with the data of V. Chabaud et al., Phys. Letters 38B, 441 (1972).
17. G. Brandenberg et al., SLAB-PUB-1203 (1973).
18. R. Anderson et al., SLAC-PUB-1178 (1973).
19. See, e.g. the review of R. Wilson, Proceedings of the 1971 International Symposium on Electron and Photon Interactions at High Energies, Cornell.
20. G. Barbiellini et al. and V. Alles-Borelli et al., reported by V. Silverstrini, to the XVI International Conference on High Energy Physics, Chicago-NAL (1972).
21. S. Brodsky and G. Farrar, SLAC-PUB-1290 (1973), to be published in Phys. Rev. Letters.
22. V. Matveev, R. Muradyan, and A. Tavkhelidze, Dubna preprint D2-7110 (1973).
23. A complete discussion of scattering amplitudes in the Bethe-Salpeter formalism is given by S. Mandelstam, Proc. Roy. Soc. (London) A233, 248 (1953). The meson Bethe-Salpeter wavefunction is the matrix element of the bilocal operator $\psi_M(x) = < M | \psi(x) \psi(0) | 0 >$. We assume that $\psi_M(x=0)$ is finite (modulo logarithms) and is non-zero, corresponding to an L = 0 bound state.
24. For the case of ladder approximation Coulomb kernel in QED, see E. Salpeter, Phys. Rev. 87, 328 (1952).
25. See S. D. Drell, and T. D. Lee, Phys. Rev. D5, 1738 (1972) and references therein.
26. For a review see S. Weinberg, paper submitted to the II Aix-en-Provence International Conference on Elementary Particles, September (1973).
27. A complete analysis of the data is given by T. Van, D. Coon, J. Gunion, and R. Blankenbecler (to be published).
28. This could happen in the model discussed by Y. Nambu in Preludes in Theoretical Physics, edited by A. de-Shalit, H. Feshback, and L. Van Hove, North-Holland Publisheding Co., Amsterdam, 1966, and H. Lipkin, Rehovot preprint, WIS 73/13 (1973).
29. This occurs in the model with ficticious colored quarks and colored gluons discussed by H. Fritzsch and M. Gell-Mann, presented to the XVI International Conference on High Energy Physics, Chicago-NAL (1972).
30. R. Blankenbecler, S. Brodsky, J. Gunion, and R. Savit, SLAC-PUB-1294 (1973), to be published in Physical Review.
31. See S. Brodsky, F. Close, and J. Gunion, Phys. Rev. D6, 177 (1972), SLAC-PUB-1243 (to be published in Phys. Rev.), and references therein.
32. R. Blankenbecler, S. Brodsky, J. Gunion, and R. Savit (to be published).
33. A rough approximation to (23) is[10]

$$\mathcal{M} = F_D(t)\, F_C(u)\, s\, F_A(s)$$

This result does not include possible logarithmic modifications which favor $\bar{x} \sim 1$ (see Ref. 12) and assumes symmetric behavior[34] in the two off-shell arguments of ϕ_A (which is the case for meson and photon scattering). Up to spin corrections, Eq. (24) has general applicability.

34. I. Muzinich and P. Fishbane, BNL preprint (1973).
35. This is of course equivalent to the important result of P. Landshoff, J. Polkinghorne, and R. Short, Nulc. Phys. B28, 225 (1971) who derive Regge behavior for $F_2(\omega)$ from the Regge behavior of the quark-proton scattering amplitude. In our terms the latter is a result of the Regge behavior of hadron-proton scattering amplitudes in the reducible contribution.
36. For reviews, see S. Drell, presented to the XVI International Conference on High Energy Physics, Chicago-NAL (1972), and J. Sullivan, presented to the SLAC Summer Institute in Particle Physics (1973).
37. J. Bjorken and J. Kogut, Phys. Rev. D8, 1341 (1973).
38. J. Bjorken, presented to the II Aix-en-Provence International Conference on Elementary Particles, September (1973).
39. Further, in order to allow for low $p_\perp$ data, we assumed mass corrections corresponding to meson form factors proportional to $1/(t - 0.71\ \text{GeV}^2)$.
40. See also Refs. 12 and 13.
41. Detailed discussions of the properties of the final state and possible jets in inclusive large transverse momentum reactions are given in J. Bjorken, SLAC-PUB-1280 (1973), J. Bjorken and G. Farrar, SLAC-PUB-1298 (1973), J. Bjorken, Ref. 38, and S. Ellis and M. Kislinger, Ref. 9.
42. Thus we predict $d\sigma/dp_\perp^2 \propto p_\perp^{-8}$ at fixed $p_\perp/\sqrt{s}$ integrated over a finite range of θ_{CM}. Here $p_\perp$ is the total transverse momentum of the hadrons produced with a minimum transverse momentum on one side of the production process.
43. As emphasized by Bjorken[38], such subprocesses have a sizeable probability to produce hadrons with all or nearly all of the jet's momentum, in contrast to mechanisms such as $qq \to qq$ or $M\bar{M} \to q\bar{q}$ which produce hadrons with a decreasing probability ($\sim (1 - x)$) to have all of the quark-jet's momentum.
44. This crucial fact and the indication that the effective trajectories decrease to negative values and are not taken into account in the models of Horn and Moshe[9], Amati et al.[13], H. Fried and T. Gaisser, Phys. Rev. D4, 3330 (1971), and Brown University preprints (1973). However, many of the techniques introduced in these papers, especially the eikonal techniques of Fried and Gaisser, are very valuable and possibly could be applied to models incorporating the scaling laws and the observed Regge behavior at large momentum transfer.
45. The derivation given in Ref. 11, shows, however, that only a few internal lines of a subprocess need transfer the high momentum; the wavefunctions of all the hadrons are not all probed simultaneously at short distance.

46. For interesting phenomenological applications, see A. Donnachie and P. R. Thomas, Daresbury preprints (1973), and R. Blankenbecler and V. Bhasin (to be published).
47. K. Johnson, Phys. Rev. D6, 1101 (1972), D. Coon, (private communication), and J. Bjorken, presented to the SLAC Summer Institute on Particle Physics (1973).
48. See, for example, G. Preparata, presented to the International Symposium on Electron and Photon Interactions at High Energies, Bonn, August (1973). A. Bramon, E. Etim, and M. Greco, Phys. Letters 41B, 609 (1972), J. Bjorken and J. Kogut, Ref. 37, and J. Sakurai, Lectures presented at the International School of Subnuclear Physics, Erice (1973).
49. Possible physical mechanisms for suppressing quark production in gauge theories are discussed by J. Bjorken, Ref. 47, A. Casher, J. Kogut, and L. Susskind, Cornell preprints CLNS 250, 251 (1973), and S. Weinberg, Ref. 26.